Nanomateriali per applicazioni high tech

nano
materials.it™

Prodotti e applicazioni

- Fotoanodi TiO_2
- Substrati colture cellulare
- Membrane PAA
- Nanofili e nanoparticelle metalliche
- Assorbitori solari

Ossido anodico nanotubolare TiO_2

Celle fotovoltaiche di terza generazione (DSSC o celle di Grätzel)

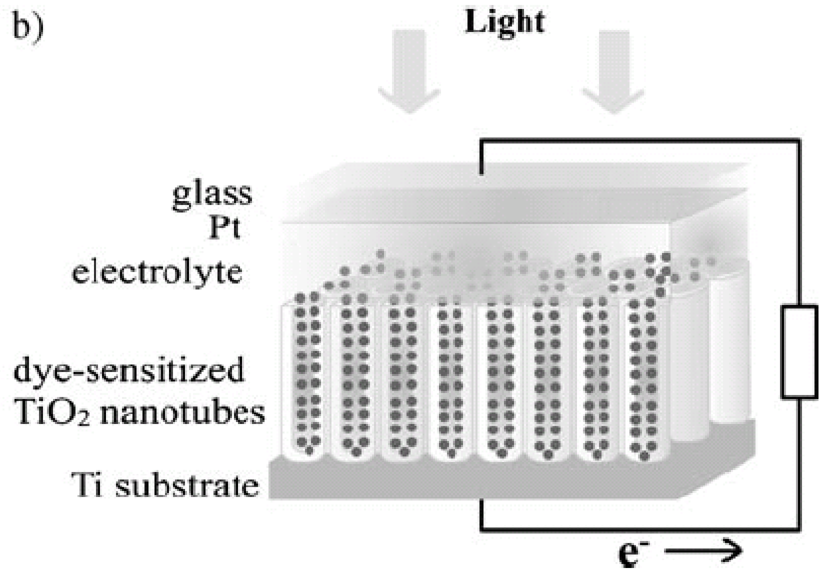

- Elettrodo ad elevata area superficiale
- Materiale semiconduttore con grande band gap ed elevata mobilità elettronica
- Minimo numero di siti di ricombinazione
- Elettrodi nanostrutturati di TiO_2, ZnO, SnO_2, …

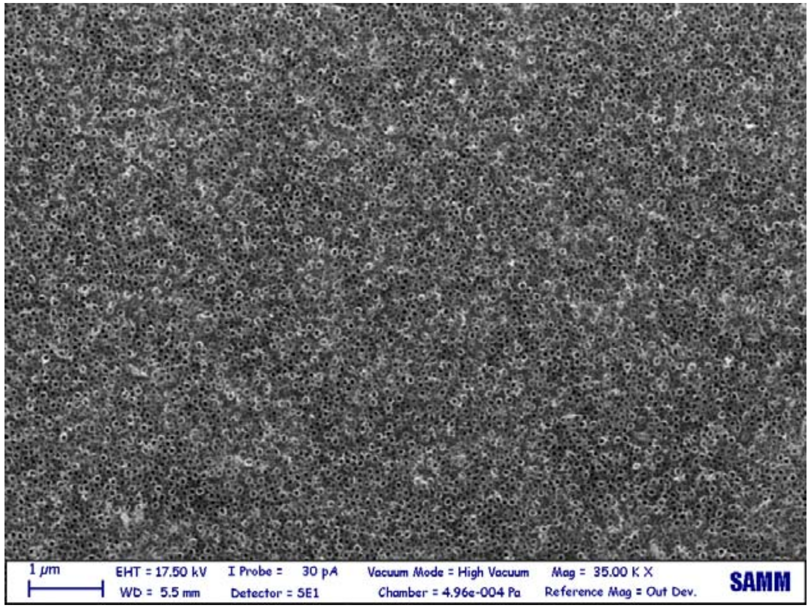

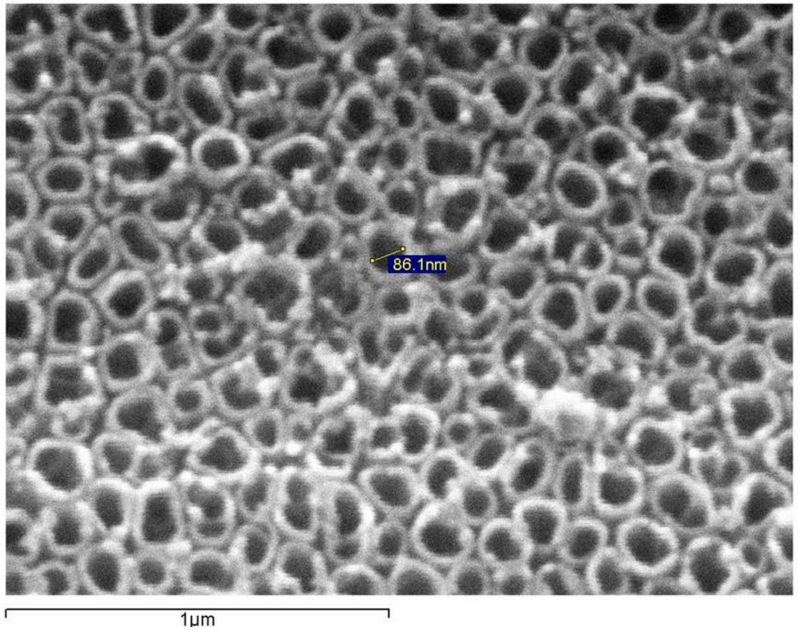

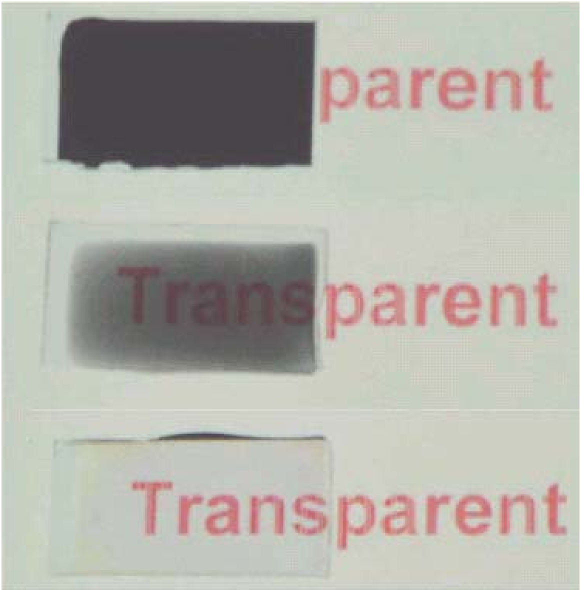

Ad oggi il fotoanodo consiste di nanoparticelle sinterizzate di TiO_2. Tuttavia è stato suggerito che la sostituzione con uno strato nanostrutturato 1D (nanofili, nanotubi, nanocolonne,…) possa migliorare le prestazioni.

Substrato per culture cellulari, cellule staminali

communications

Stem cells

TiO_2 Nanotube Surfaces: 15 nm — An Optimal Length Scale of Surface Topography for Cell Adhesion and Differentiation**

*Jung Park, Sebastian Bauer, Karl Andreas Schlegel, Friedrich W. Neukam, Klaus von der Mark, and Patrik Schmuki**

ELSEVIER

Available online at www.sciencedirect.com

ScienceDirect

Acta Biomaterialia 4 (2008) 1576–1582

Acta BIOMATERIALIA

www.elsevier.com/locate/actabiomat

Brief communication

Improved attachment of mesenchymal stem cells on super-hydrophobic TiO_2 nanotubes

Sebastian Bauer [a,1], Jung Park [b,1], Klaus von der Mark [b], Patrik Schmuki [a,*]

[a] *Department of Materials Science, WW4-LKO, Friedrich-Alexander-University of Erlangen-Nuremberg, Germany*
[b] *Department of Experimental Medicine I, Nikolaus Fiebiger-Center of Molecular Medicine, Germany*

Received 11 January 2008; received in revised form 31 March 2008; accepted 7 April 2008
Available online 25 April 2008

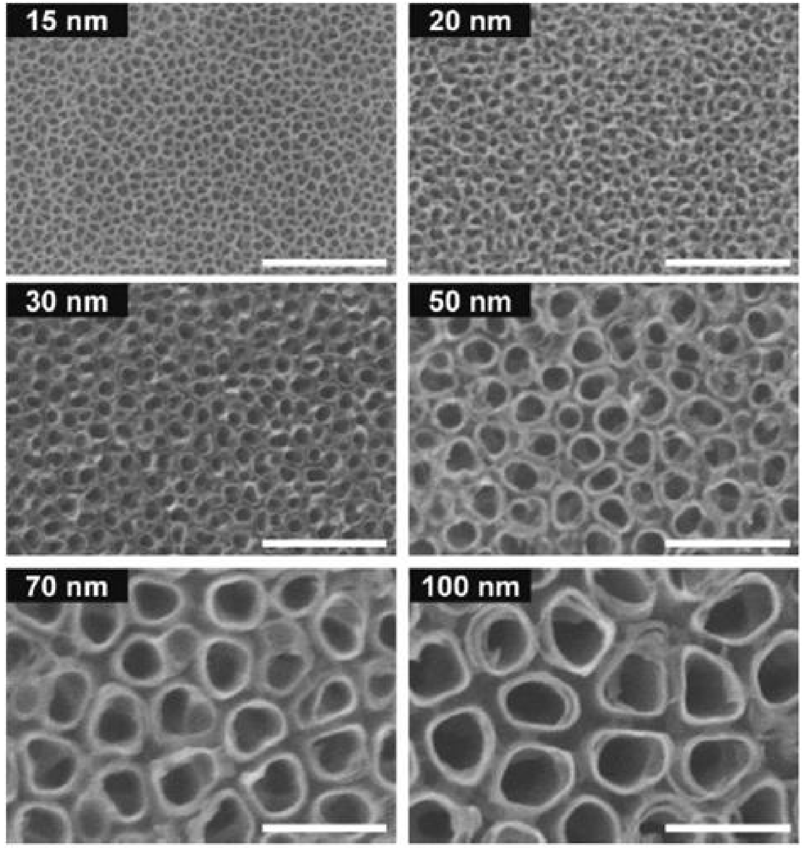

Figure 1. Top-view SEM images of self-assembled layers of vertically oriented TiO_2 nanotubes of six different diameters ranging between 15 and 100 nm formed in 1 M H_3PO_4 + 0.3 wt% HF at potentials between 1 and 20 V for 1 h. Scale bars: 200 nm.

Membrane PAA - PAT

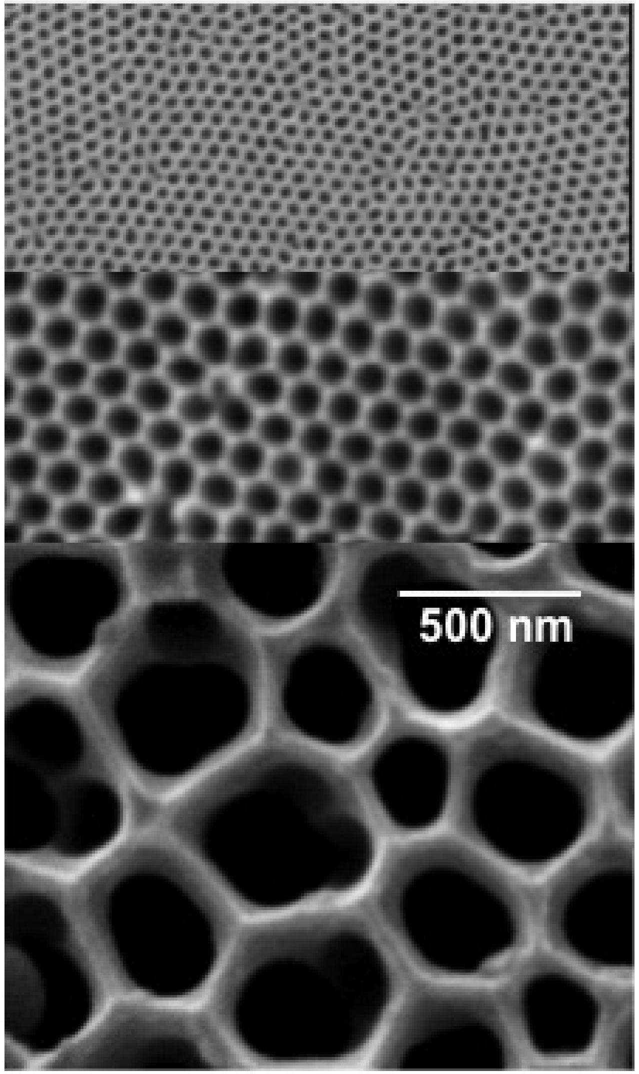

Ossidazione anodica di Alluminio 99,99X %

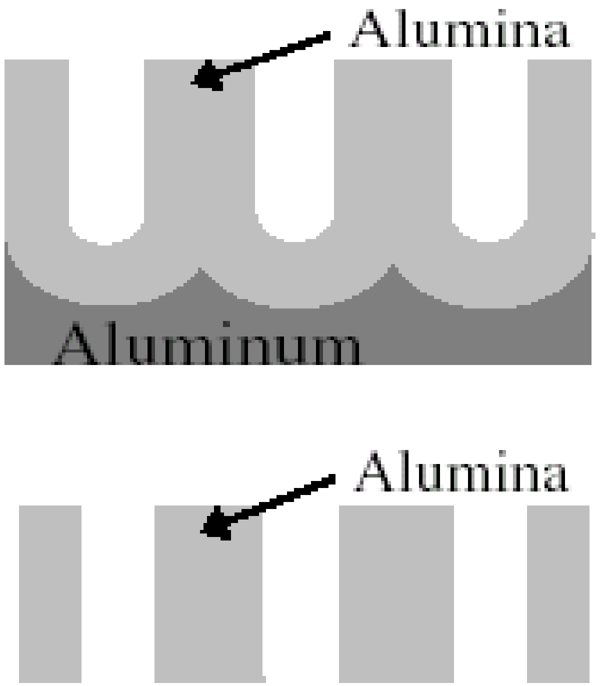

Available online at www.sciencedirect.com
SCIENCE DIRECT
Sensors and Actuators B 114 (2006) 1116–1120
SENSORS AND ACTUATORS B CHEMICAL
www.elsevier.com/locate/snb

Detection of DNA oligonucleotides on nanowire array electrodes using chronocoulometry

Aja Andreu, Jon W. Merkert, Luis A. Lecaros, Brandy L. Broglin, J. Tres Brazell, Mahnaz El-Kouedi *

Department of Chemistry, The University of North Carolina at Charlotte, Charlotte, NC 28223, USA

Received 25 March 2005; received in revised form 16 July 2005; accepted 30 July 2005
Available online 21 October 2005

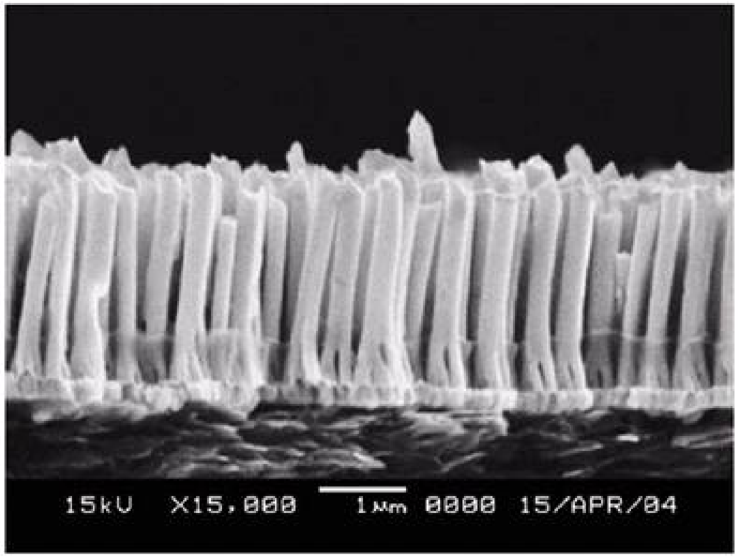

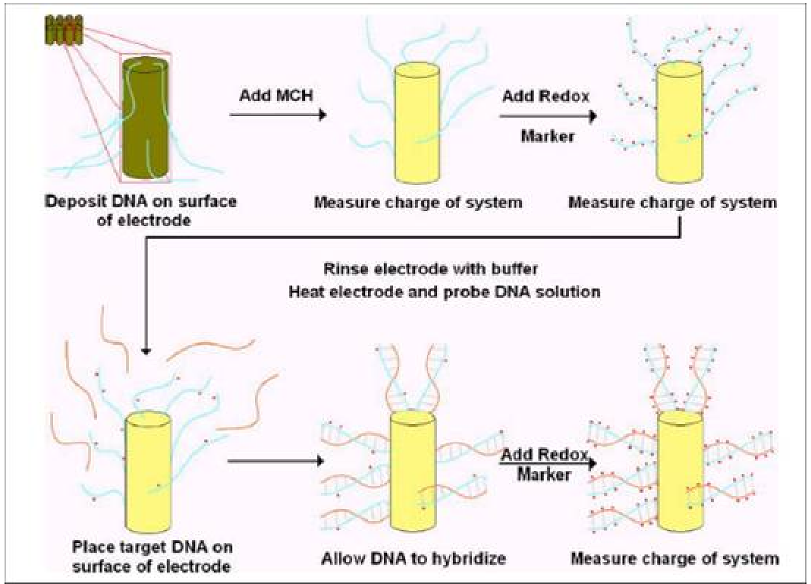

Available online at www.sciencedirect.com
ScienceDirect
Sensors and Actuators A 137 (2007) 248–255
SENSORS AND ACTUATORS A PHYSICAL
www.elsevier.com/locate/sna

A novel miniature gas ionization sensor based on freestanding gold nanowires

Ramin Banan Sadeghian*, Mojtaba Kahrizi

Department of Electrical and Computer Engineering, Concordia University, Montreal H3G1M8, Canada

Received 28 November 2006; received in revised form 8 March 2007; accepted 10 March 2007
Available online 15 March 2007

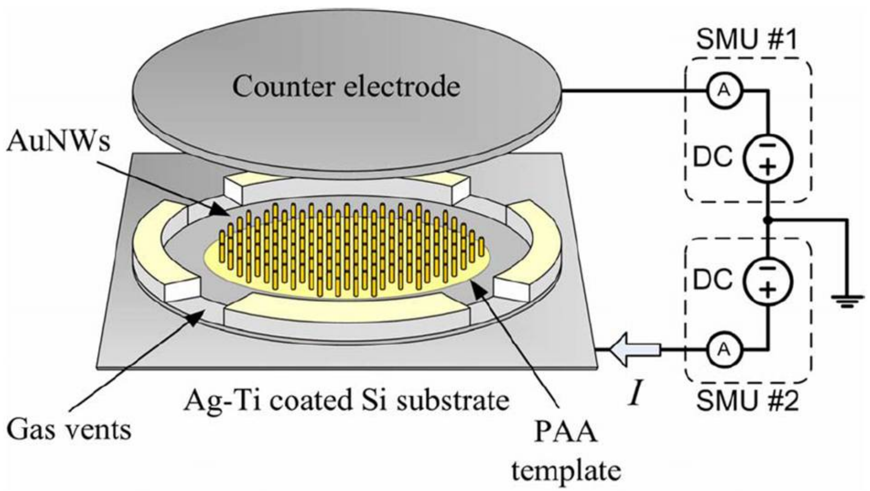

Fig. 6. Schematic illustration of the GFIS cell and the measurement setup. The counter electrode is mounted on the peripheral supporting ring. I denotes the field-ion current.

PAA per Biosensori

Available online at www.sciencedirect.com
ScienceDirect
ELSEVIER
Microporous and Mesoporous Materials 111 (2008) 359–366
MICROPOROUS AND MESOPOROUS MATERIALS
www.elsevier.com/locate/micromeso

Study on the activity and stability of urease immobilized onto nanoporous alumina membranes

Zhengpeng Yang, Shihui Si *, Chunjing Zhang

College of Chemistry and Chemical Engineering, Central South University, Changsha 410083, China

Received 26 July 2006; received in revised form 22 November 2006; accepted 10 August 2007
Available online 17 August 2007

Abstract

Nanoporous alumina membranes were employed as substrate materials for urease immobilization. Anodic porous alumina was prepared by the two-step anodization of high purity aluminum. By controlling anodization conditions, the nanoporous structure with desired dimension was obtained. Urease immobilization onto nanoporous alumina membranes was performed by four different protocols. Effect of pore diameter, pore length and immobilization methods on the activity and stability of immobilized enzyme was discussed in detail. The results show that the enzymes immobilized onto porous alumina with big pore diameter possess high activity and poor stability as compared to small pore diameter. The effect of pore length is complicated, the activity of enzyme increases with the increasing pore length for big pore size; while for correspondingly small pore size, enzymatic activity slightly depends on pore length. The immobilization methods have a slight effect on enzymatic activity, whereas enzyme immobilization by chitosan coating and reticulation with glutaraldehyde exhibits a good long-term stability as compared to that only via physical adsorption.

Keywords: Urease; Immobilization; Activity; Stability; Nanoporous alumina membranes

Catalytic nanoliths

H. Feng[d], J.W. Elam[b], J.A. Libera[b], M.J. Pellin[c], P.C. Stair[a,d,*]

[a]Department of Chemistry and Center for Catalysis and Surface Science, Northwestern University, Evanston, IL 60208, USA
[b]Energy Systems Division, Argonne National Laboratory, Argonne, IL 60439, USA
[c]Materials Science Division, Argonne National Laboratory, Argonne, IL 60439, USA
[d]Chemical Sciences and Engineering Division, Argonne National Laboratory, Argonne, IL 60439, USA

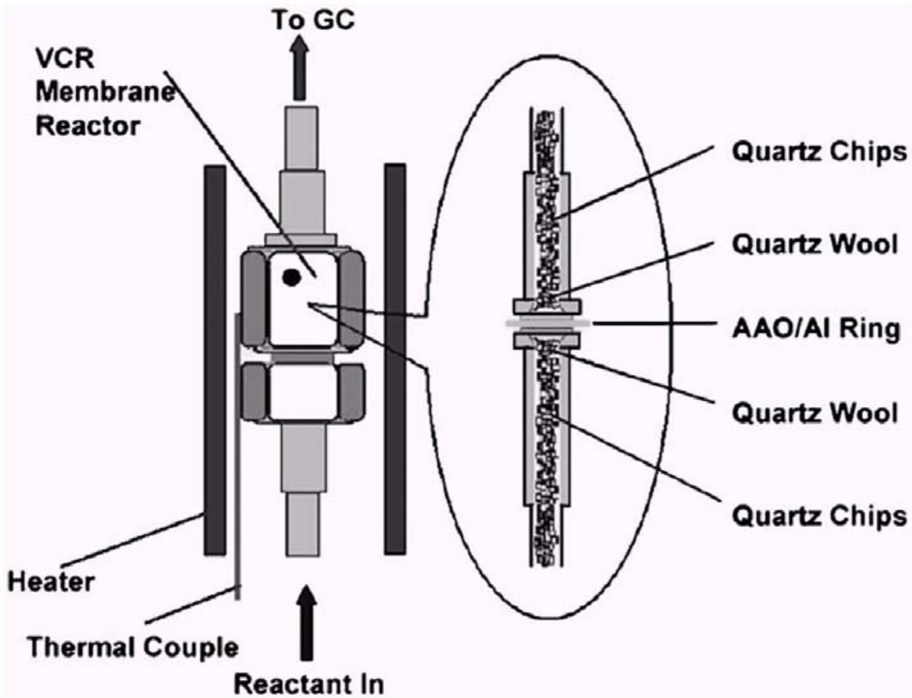

ABSTRACT: The nanoporous anodic aluminum oxide (AAO) structure is shown to be a useful platform for heterogeneous catalysis. By appropriately masking the perimeter during anodization and etching, the AAO can be formed at the center of an aluminum disc. The remaining aluminum ring connects seamlessly to the AAO and provides mechanical support for convenient handling. The supported AAO can be sealed in a standard fitting so that the nanopores in the structure function as an array of tubular reactors, i.e. a nanolith. Coating the walls with catalytically active materials turns the nanolith into a novel catalytic system.

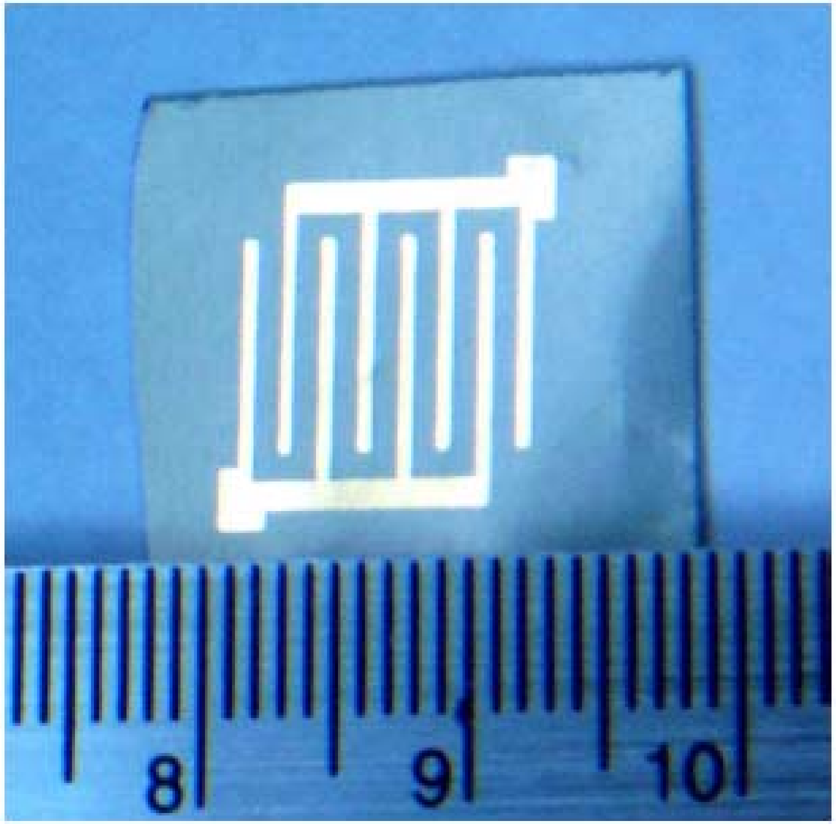

Figure 1. Digital image of a typical nanoporous alumina sensor.

Metallic Nanowires & Nanoparticles

ELSEVIER

Available online at www.sciencedirect.com
ScienceDirect

Sensors and Actuators A 137 (2007) 248–255

SENSORS AND ACTUATORS A PHYSICAL

www.elsevier.com/locate/sna

A novel miniature gas ionization sensor based on freestanding gold nanowires

Ramin Banan Sadeghian*, Mojtaba Kahrizi

Department of Electrical and Computer Engineering, Concordia University, Montreal H3G1M8, Canada

Received 28 November 2006; received in revised form 8 March 2007; accepted 10 March 2007
Available online 15 March 2007

Abstract

Freestanding gold nanowires (AuNW) were incorporated to fabricate a miniaturized gas ionization sensor. The device exhibited improved sensitivity in sub-Torr pressure (P) regime compared to similar devices reported earlier, since the room temperature breakdown voltage (V_b) was further reduced in low gas pressures or concentrations (N). Also excellent selectivity was achieved for pressures up to 10 Torr, while V_b remained almost unaffected by pressure. In the V_b–P characteristic below 1 Torr, V_b was less when the AuNWs was configured as cathode, and it started to decline until a Paschen-like $(V_b)_{min}$ was observed at very low pressures ($0.3 < P < 0.5$ Torr). The reduction of breakdown voltage in this case, was attributed to the creation of an abnormally large amount of secondary electrons at the nanowire tips due to the increase in Townsend's secondary ionization factor (ω/α) at very high reduced fields (E/N). The pre-breakdown I–V characteristic of the device, obtained at extreme low pressures showed polarity dependency. The field enhancement factor (β) of the AuNW array was estimated by operating the device in the ohmic discharge region. The average aspect-ratio of the nanowires, which was extracted from the I–V characteristic, showed good agreement with SEM observations.

Keywords: Gas ionization sensor; Gold nanowires; Breakdown voltage; Field enhancement; Sub-Torr pressure

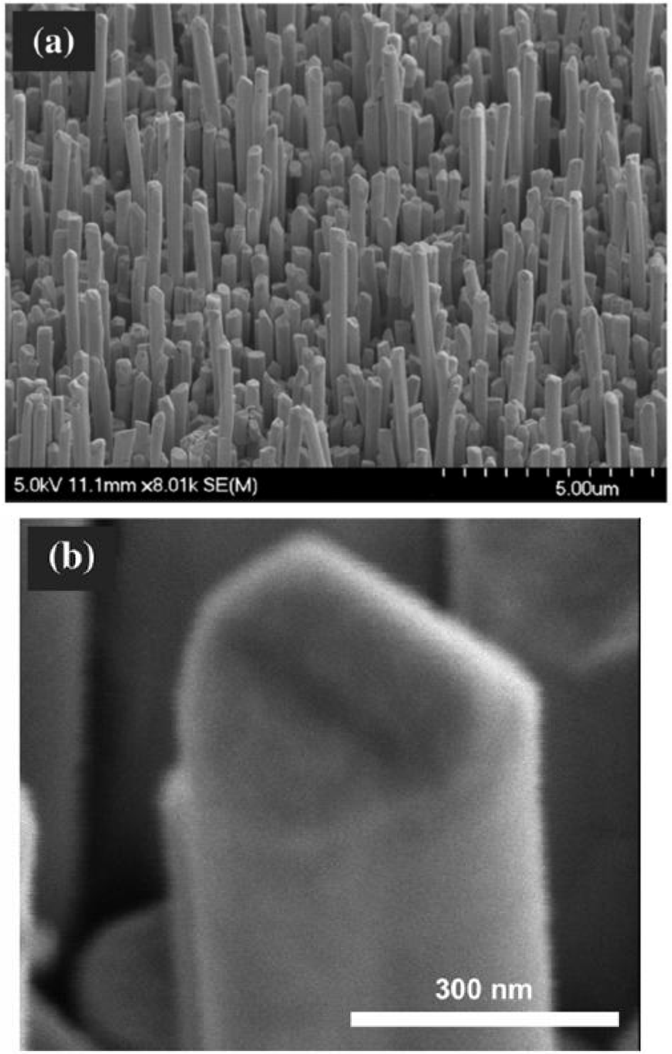

Materiali nanocompositi:
Matrice polimerica + nanofili-nanoparticelle

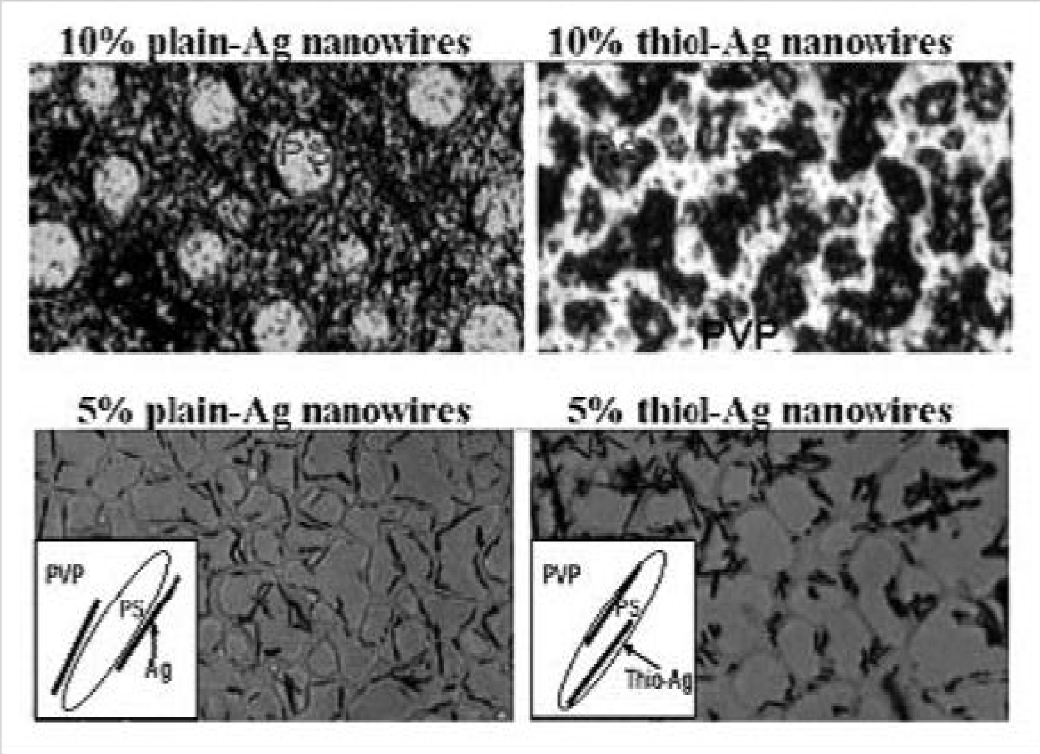

Preferential partition of silver nanowires in thin films of PS/PVP (30/70) blends at a casting temperature of −10 °C.

Electrical Conductivity in Polymer Composites Containing Metal Nanowires: Simulation and Experiment

White, Sadie; Vemulkar, Tarun; Fischer, John; Winey, Karen

American Physical Society, 2009 APS March Meeting, March 16-20, 2009, abstract #P19.008

The study of rod percolation behavior has resurfaced in recent years, because it explains electrical conductivity in polymer nanocomposites containing carbon nanotubes and metal nanowires. Common processing techniques result in fillers with L/D < 50, so traditional models, which are only strictly correct in the limit of L/D ˜∞, are ineffective at predicting percolation in these systems. We present a simulation that constructs percolated networks of finite-aspect ratio rods and calculates their electrical conductivity. We will compare our simulation results with polymer composites containing silver nanowires with aspect ratios of ˜10 and ˜30. Finally, we will present the temperature-dependent electrical conductivity of these composites and interpret the results using the thermal expansion coefficients of polystyrene and silver. These materials act as ``thermal switches,'' wherein electrical conductivity of certain composites can be manipulated by several orders of magnitude over the temperature range from 80K-425 K.

Polymer Composites with Oriented Magnetic Nanowires as Fillers

Li Sun, Kusuma Keshoju

Metallic nickel nanowires with excellent physical properties have been introduced into polydimethylsiloxane matrix to form polymer nanocomposites. Nanowires were synthesized by template-assisted electrochemical deposition. By utilizing ferromagnetic nickel nanowires, small external magnetic field can be used to control their alignment and distribution during composite synthesis. Unlike dielectrophoresis, optical tweezers, and microfluidic flow control, magnetic manipulation provides a cost-effective, non-contact, and versatile approach to control nanostructured materials in fluids over a large area. Polydimethylsiloxane composites with nanowires arranged in longitudinal, transverse, and random orientations with respect to the applied load direction were studied. Tensile tests showed that the composites with longitudinal arrangement have higher elastic modulus and tensile strength than the other composite samples. Experimentally obtained elastic modulus values were compared with the prediction of classical Halpin-Tsai model. Metallic nickel nanowires with excellent physical properties have been introduced into polydimethylsiloxane matrix to form polymer nanocomposites. Nanowires were synthesized by template-assisted electrochemical deposition. By utilizing ferromagnetic nickel nanowires, small external magnetic field can be used to control their alignment and distribution during composite synthesis. Unlike dielectrophoresis, optical tweezers, and microfluidic flow control, magnetic manipulation provides a cost-effective, non-contact, and versatile approach to control nanostructured materials in fluids over a large area. Polydimethylsiloxane composites with nanowires arranged in longitudinal, transverse, and random orientations with respect to the applied load direction were studied. Tensile tests showed that the composites with longitudinal arrangement have higher elastic modulus and tensile strength than the other composite samples. Experimentally obtained elastic modulus values were compared with the prediction of classical Halpin-Tsai model.

•Nanoparticles

•Nanorods

•Nanowires

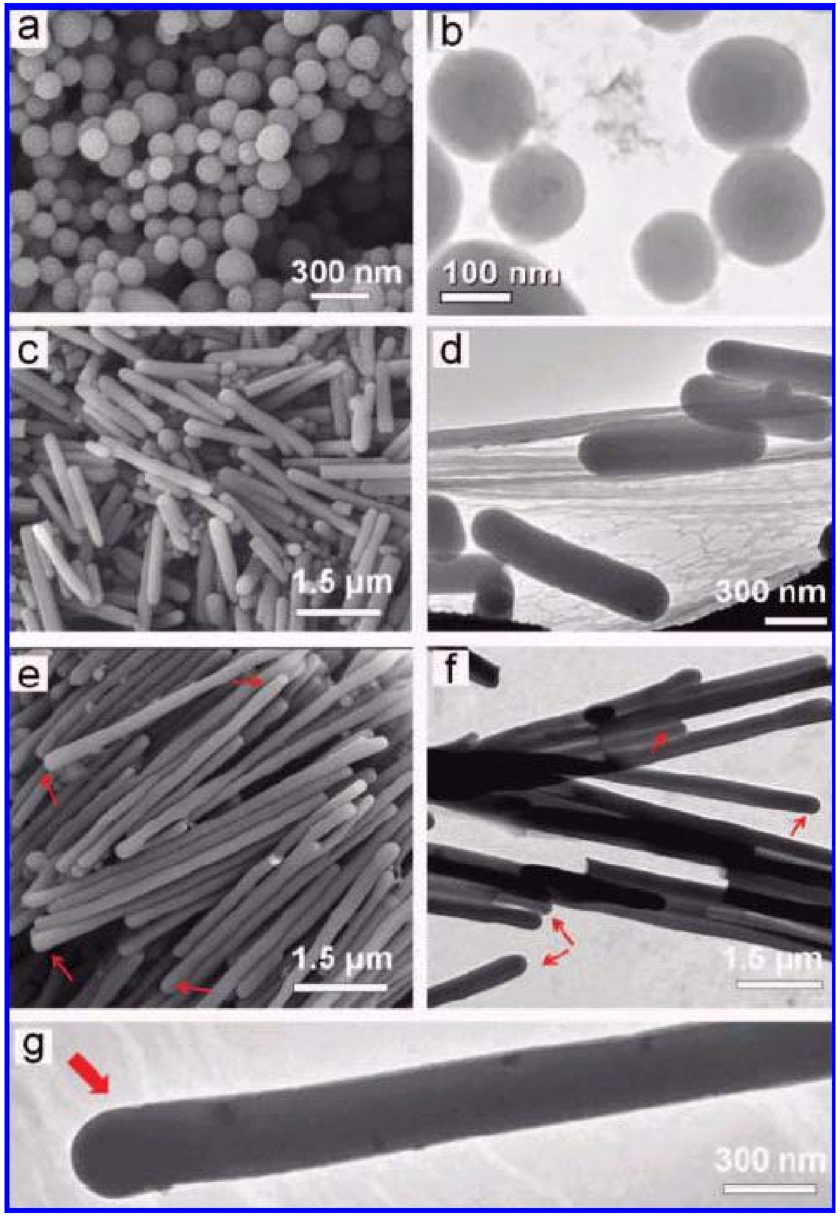

Supporti nanostrutturati per Assorbitori Solari

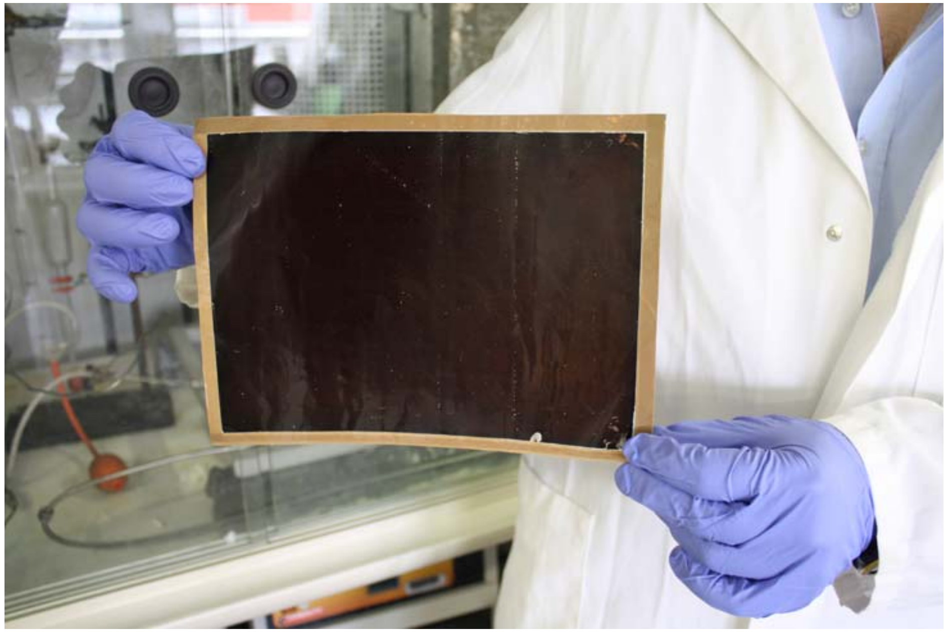

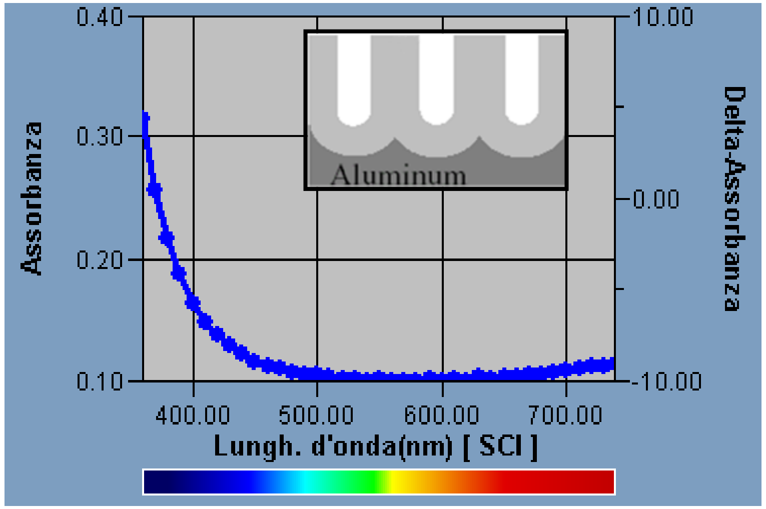

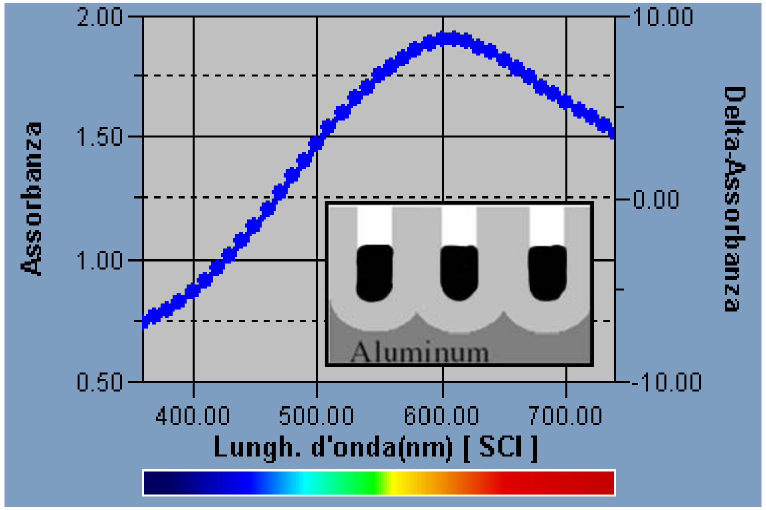

Membrana PAA Ø 90 mm

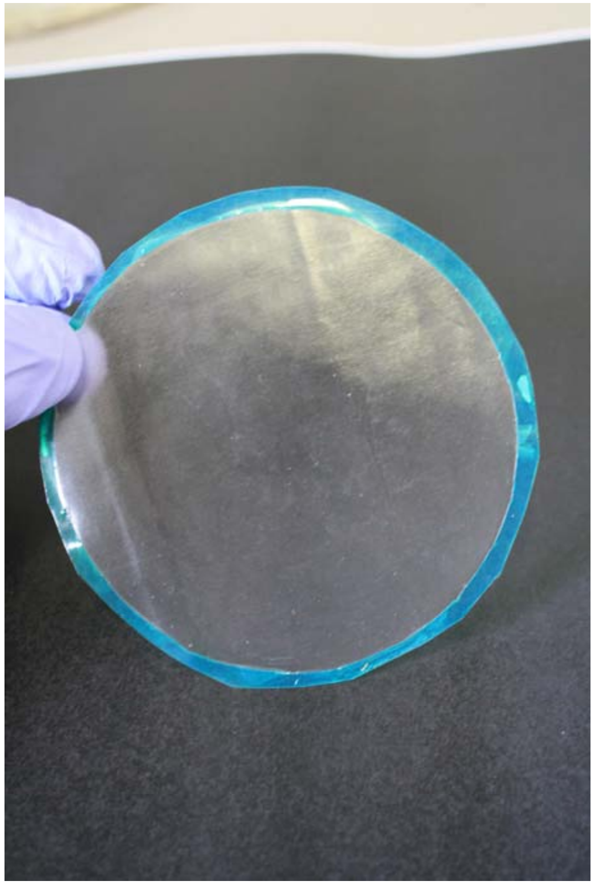

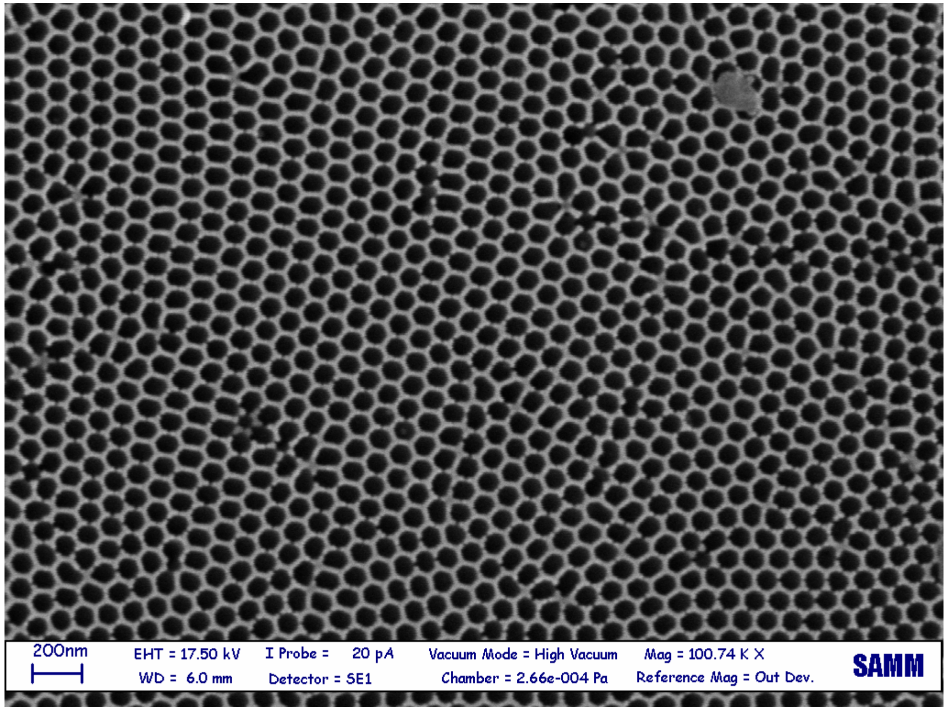

Cu NWs in PPA

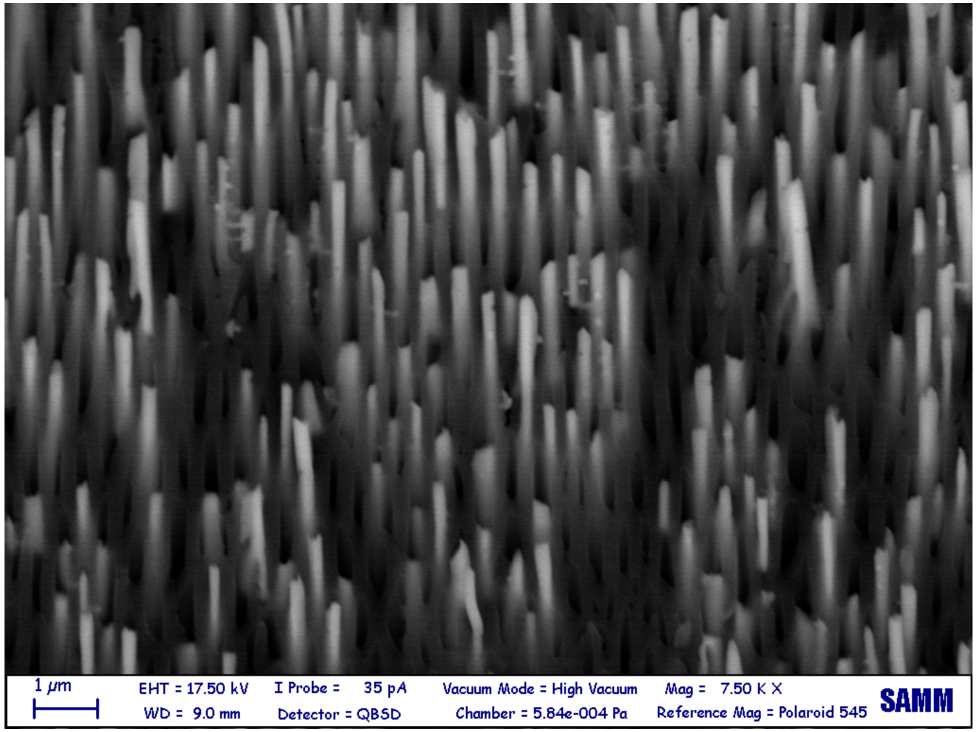

Cu NWs in PPG

Soluzioni Ag Nanoparticles

Ø

4 → 20 nm

FINE